Theoretical x-ray transition probabilities for high-Z superheavy elements*

R. Anholt†
Department of Chemistry and Yale Heavy Ion Accelerator Laboratory, Yale, New Haven, Connecticut 06520

J. O. Rasmussen‡
Department of Chemistry and Lawrence Berkeley Laboratory, University of California, Berkeley, California 94720
(Received 10 September 1973)

K and L x-ray transition probabilities have been calculated for several elements between $Z=92$ and 170. The calculations include multipoles higher than $E1$, are relativistic, and utilize Dirac-Hartree-Fock wave functions with finite-size nuclei. At these very high atomic numbers many transition rates go through a maximum as a function of Z, and other transitions show a maximum and a minimum, and then begin to increase again past $Z=150$.

I. INTRODUCTION

Of late, considerable interest has developed in the binding energies and x-ray transitions in elements of very high atomic number. Much of this interest is in the region of $Z=170$, where the K-shell binding energy drops into the positron continuum. Müller *et al.* have suggested that at around this atomic number, a K-shell vacancy may decay by autoionizing a positron and that this process may compete favorably with normal radiative and Auger mechanisms of decay.[1] Both Greiner's group[2] and Popov[3] have made calculations to show where the K-shell energy drops into the positron continuum, and this work has raised a number of questions as to what sort of Hamiltonian and quantum-electrodynamic terms are required at these very high fields in order to accurately predict binding energies.

To answer these kinds of questions, x-ray energies and transition strengths are important. Unfortunately, even if synthesis of nuclei with atomic number greater than 130 is achieved, these nuclei will probably be so short-lived and in such low yield that x rays cannot be observed in the stationary atom. There is, however, the possibility of observing united-atom x rays during a collision between a high-energy heavy ion and a neutral atom.

In this respect we mention work of Mokler, Stein, and Armbruster[4] and Gove, Jundt, and Kubo,[5] who claim to have observed Mx rays of $Z=132$, 143, and 145 during a 10–60-MeV I bombardment of Au, Th, and U targets. With new heavier ion capabilities of several accelerators throughout the world, there is the possibility of carrying such experiments further to see evidence of M-, L-, or K-shell transitions up to united atom total charge as high as 190. Therefore, it seemed of value to us to carry out theoretical calculations of radiative transition rates for very high atomic numbers.

Previously, there have been almost no transition probabilities calculated for any element above $Z=93$, though a considerable number have been made for elements below that atomic number. The earliest relativistic calculations were done by Payne and Levinger[6] and later Payne and Taylor,[7] who employed analytical Dirac wave functions with screening to calculate K transition rates in a number of elements up through lead. Babuskin[8] similarly used analytical Dirac wave functions, but in addition, he used a more sophisticated expression for the electric and magnetic multipole fields, and even investigated the inclusion of finite nuclear size in his calculations. His work, while being analytically more elegant than subsequent work, has largely been superseded by approaches which use computer-calculated Hartree-Fock many-electron wave functions instead of one-electron Dirac functions.

Among these are the calculations of three groups, Rosner and Bhalla,[9] Scofield,[10] and Lu, Malik, and Carlson.[11] We have followed their approach closely herein and we discuss it below.

II. RELATIVISTIC FORMULATION OF TRANSITION RATES

As usual for quantum mechanical transition probabilities we begin with the Fermi Golden Rule, writing the transition rate ω as

$$\omega = 2\pi S|\langle f|H_{\text{int}}|i\rangle|^2\rho(E_f)\ , \tag{1}$$

where S stands for the summation over final and average over initial states, and we have taken atomic units throughout ($\hbar=m=e=1$). H_{int} in this analysis will be taken as

$$H_{\text{int}} = \sum_{i=1}^{N} \vec{J}_i \cdot \vec{A}\ , \tag{2}$$

with $\vec{J} = c\vec{\alpha}$, $\vec{\alpha}$ being the usual Dirac matrix. For the $\vec{A}$ field we take the sum over electric and magnetic multipolarities expressed as

$$A^{(e)}_{L,M} = \left(\frac{4\pi\omega}{R}\right)^{1/2}\left[\left(\frac{L+1}{2L+1}\right)^{1/2} j_{L-1}(\omega r)T^{M}_{L,L-1}(\theta,\phi) - \left(\frac{L}{2L+1}\right)^{1/2} j_{L+1}(\omega r)T^{M}_{L,L+1}(\theta,\phi)\right] \tag{3}$$

and

$$A^{(m)}_{L,M} = \left(\frac{4\pi\omega}{R}\right)^{1/2}\left[-j_L(\omega r)T^{M}_{L,L}(\theta,\phi)\right],$$

with $j_L(\omega r)$ the spherical Bessel functions of the first kind and $T^{M}_{L,L}$ spherical tensors defined by Rose.[12]

The wave functions in this analysis can be expressed as

$$\psi^{\mu}_{\kappa} = \begin{pmatrix} G/r & \chi^{\mu}_{\kappa} \\ iF/r & \chi^{\mu}_{-\kappa} \end{pmatrix}, \tag{4}$$

where κ is the usual relativistic quantum number ($\kappa = l$ for $\kappa > 0$, $\kappa = -l-1$ for $\kappa < 0$). Performing the necessary algebra, we then have for the magnetic and electric transition rates between final and initial states labeled with and without a prime, respectively:

$$\omega_{\kappa\kappa'}(ML) = 2\omega(\kappa+\kappa')^2\{(2\bar{l}'+1)(2l+1)(2j'+1)/L(L+1)\}^{-1} C^2(l\bar{l}'L;000)W^2(jlj'\bar{l}';\tfrac{1}{2}L) \times\left(\int_0^\infty (G_\kappa F_{\kappa'} + F_\kappa G_{\kappa'})j_L(\omega r)dr\right)^2, \tag{5a}$$

$$\omega_{\kappa\kappa'}(EL) = 2\omega[(2l'+1)(2l+1)(2j'+1)/(2L+1)^2]C^2(ll'L;000)W^2(jlj'l';\tfrac{1}{2}L) \times\left[\left(\frac{L+1}{L}\right)^{1/2}\int_0^\infty [(\kappa'-\kappa)(G_\kappa F_{\kappa'} + F_\kappa G_{\kappa'}) + L(G_\kappa F_{\kappa'} - F_\kappa G_{\kappa'})]\, j_{L-1}(\omega r)dr - \left(\frac{L}{L+1}\right)^{1/2}\int_0^\infty [(\kappa'-\kappa)(G_\kappa F_{\kappa'} + F_\kappa G_{\kappa'}) - (L+1)(G_\kappa F_{\kappa'} - F_\kappa G_{\kappa'})]\, j_{L+1}(\omega r)dr\right]^2, \tag{5b}$$

where α is the fine-structure constant, $\omega = \alpha(E_f - E_i)$ in atomic units, and $\bar{l}'$, in the notation introduced by Rose,[13] is taken as $-\kappa'$ for $\kappa' < 0$ or $\kappa' - 1$ for $\kappa' > 0$.

We mention at this point that the choice of the field here is arbitrary and we could just as well, following Scofield, have taken for the electric field

$$A^{(e)}_{LM} = \left(\frac{4\pi\omega}{R}\right)^{1/2}[L(L+1)]^{-1/2}\vec{\nabla}\times\vec{L}j_L(\omega r)Y_{LM}(\hat{r}),$$

in which case we would obtain for the transition rate

$$\omega_{\kappa\kappa'}(EL) = 2\omega[(2l'+1)(2l+1)(2j'+1)/L(L+1)] \times C^2(ll'L;000)W^2(jlj'l';\tfrac{1}{2}L) \times\left(\int_0^\infty dr\{j_{L-1}(\omega r)[(\kappa'-\kappa)(F_\kappa G_{\kappa'} + G_\kappa F_{\kappa'}) - L(F_\kappa G_{\kappa'} - G_\kappa F_{\kappa'})] + L(G_\kappa G_{\kappa'} + F_\kappa F_{\kappa'})j_L(\omega r)\}\right)^2. \tag{6}$$

The details of the relativistic Hartree-Fock-Slater (RHFS) calculations used by Bhalla, by Scofield, and by Lu, Malik, and Carlson do not differ by very much. They all employ the usual Slater approximation to the exchange term,

$$V_s = \frac{3\alpha}{2\pi}[3\pi^2\rho(r)]^{1/3},$$

and with the exception of Scofield's calculation, they take account of finite nuclear size (though in various different ways). For our calculations, we have used wave functions from Mann at the Los Alamos Scientific Laboratory. These wave functions are based on a Dirac-Hartree-Fock (DHF) code[14] which calculates the many two-electron exchange integrals exactly. The finite nuclear size is taken as a two parameter Fermi distribution with $R = 1.07A^{1/3}$ fm, $a = 1.0393\times10^{-5}$ a.u., and $A = 3Z - 46$. More-sophisticated extrapolations for A yielded results which were not too much different from those used in this calculation.[15]

For the matrix elements necessary to calculate transition probabilities, we integrated along the same exponential radial grid as was used to calculate the self-consistent field. In such a grid each r_i is given as $r_i = r_0 e^{hi}$ with $r_0 = 5\times10^{-5}$ a.u. and h is selected to give a maximum radius of 40 a.u. at $i = 421$. We found that interpolating the wave functions at linear intervals of 0.001, 0.01, and 0.000 01 a.u. when the exponential grid was wider than this did not change the value of the matrix elements by more than 0.5%.

For the x-ray transition energy, we have taken the difference between Mann's eigenvalues. Lu,

TABLE I. Comparison of K-shell radiative transition rates for $Z=92$ and 126.

Author	K-L_1	K-L_2	K-L_3	K-M_2	K-M_3	K-M_4	K-M_5	K-N_2	K-N_3	K-N_4	K-N_5
						$Z=92$					
Bhalla [a]	0.0043	1.056	1.681	0.194	0.381	0.006 97	0.0079	0.049	0.099	0.0021	0.0024
Scofield [b]	0.0038	1.01	1.622	0.187	0.366	0.0065	0.0075	0.047	0.095	0.0019	0.0022
LMC [c]	0.0038	1.01	1.62	0.187	0.366	0.0065	0.0074	0.047	0.095	0.0019	0.0022
This work	0.0037	1.005	1.602	0.186	0.362	0.006 44	0.0073	0.046	0.093	0.0019	0.0022
						$Z=126$					
LMC [c]	0.189	3.71	4.66	0.495	1.23	0.037	0.030	0.124	0.373	0.0133	0.0116
This work [d]	0.19	3.6	4.6	0.485	1.22	0.037	0.031	0.12	0.37	0.0133	0.0115

[a] Results are for $Z=93$, so they are consistently higher than others, Ref. 9.
[b] Reference 10.
[c] Reference 11.
[d] Interpolated.

Malik, and Carlson[11,16] examined the error associated with this approximation for $Z=92$ and 126. They used experimental data extrapolating a curve that goes approximately as Z^4 up to $Z=126$, to find the correction due to quantum electrodynamic and other terms. When this correction was applied to the differences between eigenvalues, and the x-ray transition probabilities were recalculated, the difference in the rates was on the order of 0.1%. The difference between the energies was around 0.5%, and we note from extrapolating the curves even further, that this does not become much greater as one approaches $Z=200$.

We mention one other source of error, which is in not taking the initial and final wave functions with a hole in the appropriate shells. The wave functions we have taken are for the neutral atoms. Lu, Malik, and Carlson have examined this source of error for $Z=92$ and 126 K x-ray transition-rate calculations. They found the difference in the transition rates to be on the order of 1 or 2%, the hole wave-function rates giving consistently higher rates. Again, however, these do not become drastically larger than 1 or 2% as one goes to

TABLE II. Comparison of intensity ratios with experiment for $Z=92$.

Ratio	Experiment [a]	This work	Scofield
$K\alpha_2/K\alpha_1$	0.624	0.627	0.623
$K\beta_3/K\beta_1$	0.548	0.513	0.510
$(K\beta_1+K\beta_3)/K\alpha_1$	0.354	0.342	0.341
$K\beta_1'/K\alpha_1$	0.363	0.351	0.350
$K\beta_2'/K\alpha_1$	0.123	0.0861 [b]	0.087 [b]
$K\beta/K\alpha$	0.299	0.272 [b]	0.270 [b]
$L\beta_4/L\beta_3$	1.10	1.15	1.15
$L\gamma_3/L\beta_3$	0.438	0.310	0.310
$L\gamma_2/L\beta_3$	0.402	0.308	0.313
$L\eta/L\beta_1$	0.0280	0.0286	0.0284
$L\gamma_1/L\beta_1$	0.240	0.226	0.226
$L\beta_{2,15}/L\alpha_1$	0.275	0.233	0.233
$L\alpha_2/L\alpha_1$	0.110	0.114	0.114
$L\beta_6/L\beta_1$	0.0185	0.0175	0.0174

[a] Experimental data taken from a recent compilation by Salem and Schultz (Ref. 19) and Nelson, Saunders, and Schultz (Ref. 20). X-ray notation used here is explained therein. The estimated experimental uncertainties ranged from 3 to 10%.
[b] Included in $K\beta_2'$ and $K\beta$ are transitions from higher levels that were not calculated theoretically.

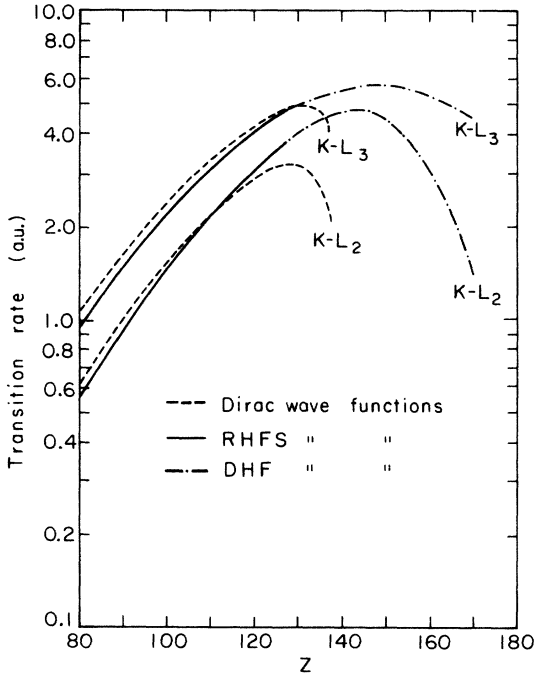

FIG. 1. K-L_3 and K-L_2 transition rates vs Z. Calculations made by Lu, Malik, and Carlson (Ref. 11) using RHFS wave functions, and by ourselves, using hydrogenic Dirac wave functions and Mann's many-electron Dirac-Hartree-Fock wave functions.

TABLE III. Transition rates (a.u.).

	To the K shell													
Z	L_1 $M1$	L_2 $E1$	L_3 $E1/M2$	M_1 $M1$	M_2 $E1$	M_3 $E1/M2$	M_4 $E2/M1$	M_5 $E2/M3$	N_1 $M1$	N_2 $E1$	N_3 $E1/M2$	N_4 $E2/M1$	N_5 $E2/M3$	N_6 $M2$
92	0.3734(−2)	0.1005(1)	0.1602(1)	0.1196(−2)	0.1859(0)	0.3619(0)	0.6438(−2)	0.7334(−2)	0.3445(−3)	0.4589(−1)	0.9344(−1)	0.1891(−2)	0.2161(−2)	0.1621(−8)
112	0.4009(−1)	0.2308(1)	0.3234(1)	0.1293(−1)	0.3845(0)	0.7968(0)	0.2028(−1)	0.1984(−1)	0.3981(−2)	0.9895(−1)	0.2285(0)	0.6871(−2)	0.6813(−2)	0.2899(−7)
130	0.2866(0)	0.4121(1)	0.4955(1)	0.8868(−1)	0.4930(0)	0.1339(1)	0.4117(−1)	0.3338(−1)	0.2783(−1)	0.1194(0)	0.4126(0)	0.1526(−1)	0.1268(−1)	0.2015(−6)
150	0.1989(1)	0.4623(1)	0.5779(1)	0.5259(0)	0.2680(−1)	0.1775(1)	0.5684(−1)	0.3485(−1)	0.1600(0)	0.7280(−3)	0.5837(0)	0.2284(−1)	0.1449(−1)	0.9233(−6)
160	0.4273(1)	0.2916(1)	0.5315(1)	0.1002(1)	0.1600(0)	0.1755(1)	0.5288(−1)	0.2777(−1)	0.2948(0)	0.6433(−1)	0.5955(0)	0.2204(−1)	0.1204(−1)	0.1482(−5)
170	0.7641(1)	0.1440(1)	0.4514(1)	0.1615(1)	0.6219(0)	0.1605(1)	0.4304(−1)	0.1946(−1)	0.4591(0)	0.1799(0)	0.5623(0)	0.1862(−1)	0.8792(−2)	0.1967(−5)
	To the L_1 shell													
Z	L_2 $E1$	L_3 $E1/M2$	$M1$ $M1$	M_2 $E1$	M_3 $E1/M2$	M_4 $E2/M1$	M_5 $E2/M3$	N_1 $M1$	N_2 $E1$	N_3 $E1/M2$	N_4 $E2/M1$	N_5 $E2/M3$		
92	0.1114(−5)	0.5026(−2)	0.1790(−5)	0.3103(−1)	0.2698(−1)	0.1477(−2)	0.2194(−2)	0.8464(−6)	0.8314(−2)	0.8367(−2)	0.2544(−3)	0.4059(−3)		
112	0.4944(−5)	0.4783(−1)	0.2805(−4)	0.1006(0)	0.3772(−1)	0.7189(−2)	0.1040(−1)	0.1385(−4)	0.2829(−1)	0.1470(−1)	0.1508(−2)	0.2403(−2)		
130	0.1857(−2)	0.3417(0)	0.3213(−3)	0.3039(0)	0.9804(−2)	0.2707(−1)	0.3655(−1)	0.1598(−3)	0.8273(−1)	0.7513(−2)	0.6879(−2)	0.1031(−1)		
150	0.2597(−1)	0.2430(1)	0.5225(−2)	0.1257(1)	0.1400(0)	0.1043(0)	0.1186(0)	0.2428(−2)	0.2542(0)	0.2601(−1)	0.3266(−1)	0.4078(−1)		
160	0.2934(0)	0.5168(1)	0.2003(−1)	0.2289(1)	0.6147(0)	0.1831(0)	0.1827(0)	0.8724(−2)	0.3414(0)	0.1540(0)	0.6219(−1)	0.6790(−1)		
170	0.1350(1)	0.9057(1)	0.6846(−1)	0.3560(1)	0.1525(1)	0.2913(0)	0.2499(0)	0.2783(−1)	0.3737(0)	0.4293(0)	0.1051(0)	0.9892(−1)		
	To the L_2 shell													
Z	L_3 $E2/M1$	M_1 $E1$	M_2 $M1$	M_3 $E2/M1$	M_4 $E1/M2$	M_5 $M2$	N_1 $E1$	N_2 $M1$	N_3 $E2/M1$	N_4 $E1/M2$	N_5 $M2$			
92	0.2361(−3)	0.3412(−2)	0.5010(−6)	0.1749(−3)	0.1189(0)	0.1052(−4)	0.9148(−3)	0.1997(−6)	0.5258(−4)	0.2696(−1)	0.3269(−5)			
112	0.2396(−3)	0.9882(−2)	0.7851(−5)	0.7169(−3)	0.3020(0)	0.8242(−4)	0.2844(−2)	0.3516(−5)	0.2456(−3)	0.8108(−1)	0.2966(−4)			
130	0.3587(−2)	0.2229(−1)	0.9964(−4)	0.2268(−2)	0.5688(0)	0.4421(−3)	0.6727(−2)	0.4518(−4)	0.8585(−3)	0.1763(0)	0.1746(−3)			
150	0.7150(−1)	0.1631(−1)	0.2591(−2)	0.1884(−1)	0.6662(0)	0.2292(−2)	0.5879(−2)	0.1012(−2)	0.6272(−2)	0.2464(0)	0.9703(−3)			
160	0.2440(0)	0.4033(−3)	0.1184(−1)	0.6697(−1)	0.4842(0)	0.3920(−2)	0.1260(−4)	0.3941(−2)	0.2192(−1)	0.1938(0)	0.1708(−2)			
170	0.5435(0)	0.6978(−1)	0.3540(−1)	0.1645(0)	0.3177(0)	0.5001(−2)	0.1436(−1)	0.1024(−1)	0.5520(−1)	0.1353(0)	0.2248(−2)			
	To the L_3 shell													
Z	M_1 $E1/M2$	M_2 $E2/M1$	M_3 $E2/M1$	M_4 $E1$	M_5 $E1/M2$	N_1 $E1/M2$	N_2 $E2/M1$	N_3 $E2/M1$	N_4 $E1$	N_5 $E1/M2$				
92	0.6109(−2)	0.8425(−4)	0.7053(−4)	0.1003(−1)	0.8796(−1)	0.1541(−2)	0.1682(−4)	0.1953(−4)	0.2026(−2)	0.1849(−1)				
112	0.1999(−1)	0.2730(−3)	0.2724(−3)	0.2378(−1)	0.2076(0)	0.5079(−2)	0.5022(−4)	0.7883(−4)	0.5223(−2)	0.4917(−1)				
130	0.4358(−1)	0.5277(−3)	0.7183(−3)	0.4464(−1)	0.3888(0)	0.9879(−2)	0.9363(−4)	0.2252(−3)	0.1011(−1)	0.9903(−1)				
150	0.4223(−1)	0.3296(−3)	0.1866(−2)	0.7968(−1)	0.6930(0)	0.4097(−2)	0.8760(−3)	0.6111(−3)	0.1805(−1)	0.1870(0)				
160	0.1829(−1)	0.8503(−1)	0.2872(−2)	0.1027(0)	0.8933(0)	0.6182(−4)	0.2138(−2)	0.9740(−3)	0.2301(−1)	0.2473(0)				
170	0.2044(−2)	0.5894(−2)	0.4398(−2)	0.1302(0)	0.1133(1)	0.1122(−1)	0.3536(−2)	0.1535(−2)	0.2866(−1)	0.3218(0)				

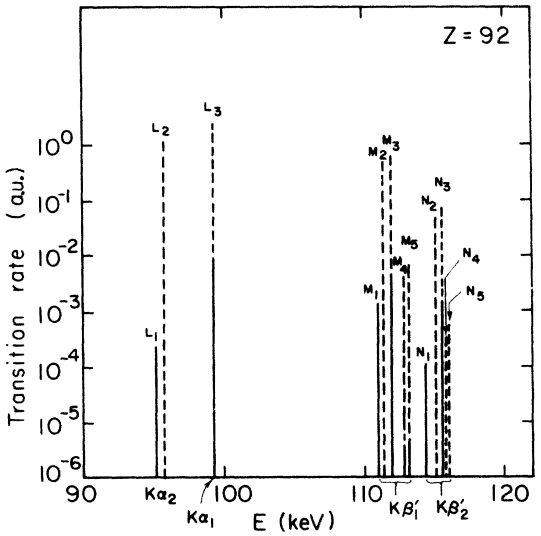

FIG. 2. Transition rate vs E histogram for $Z=92$. Magnetic contribution to transition rate is drawn as solid line; the remaining contribution is drawn as dashed line. Multipoles calculated are given in Table III.

higher Z. Furthermore, it is not to be expected that ionization of shells outside the shells involved in the transition will much affect the rate. As the work of Watson and Rasmussen[17] showed, the K x-ray energies were hardly affected by extensive ionization in fission fragments, and by the same token removal of outer-shell electrons will not much affect inner-shell wave functions.

III. NUMERICAL RESULTS

Table I gives a comparison between transition rates for $Z=92$ and 126 calculated by Bhalla, by

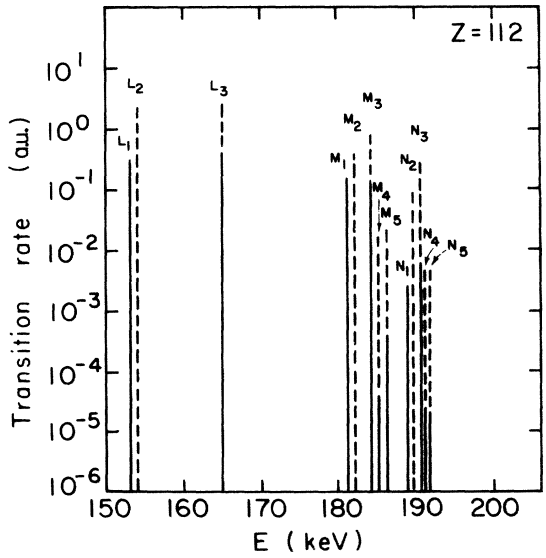

FIG. 3. Same as Fig. 2 for $Z=112$.

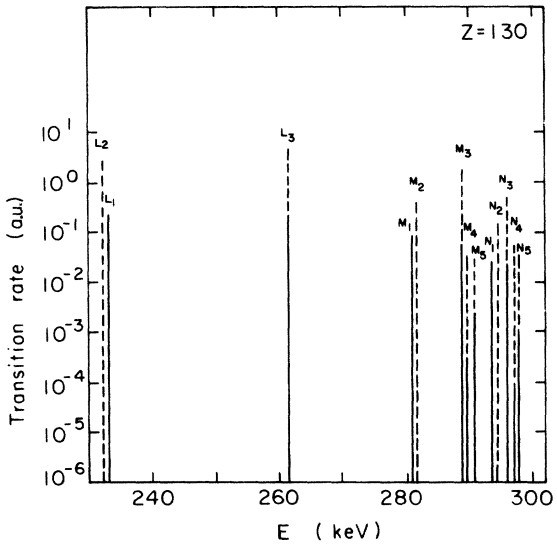

FIG. 4. Same as Fig. 2 for $Z=130$.

Scofield, by Lu, Malik, and Carlson, and by ourselves. The units used throughout are atomic rate units (1 a.u. $=4.132\times10^{16}$ sec^{-1}). In all cases, these four agree within a few percent.

One would like to compare these calculated transition rates with experimental quantities. Of course, this is at present impossible with the superheavy elements. However, it is possible to make comparisons with experimental data for the lighter elements. Scofield has compared the total K emission rates with experimental quantities for 10 elements between $Z=16$ and 79, and the agreement appeared to be within the experimental uncertainties. Dittner and Bemis[18] have compared the relative intensities of some K x rays with Lu, Malik, and Carlson's calculations for $Z=96$–99, and there too, the results agreed with theory.

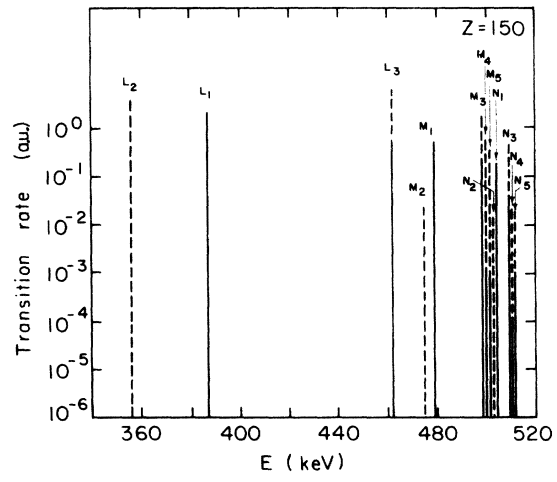

FIG. 5. Same as Fig. 2 for $Z=150$.

Ratios between various line intensities may also be compared, as is done for various K and L transitions in Table II. Even here, the agreement is fairly good, though some of the L ratios are off by as much as 20%.

Figure 1 is a plot of the transition rate versus Z for K-L_2 and K-L_3 (i.e., $K\alpha_2$ and $K\alpha_1$) transitions and compares our calculations with Lu, Malik, and Carlson's (the two curves cannot be resolved on the plot). Also plotted are our calculations made using analytical one-electron Dirac wave functions found in Ref. 12 [assuming a point nucleus, no screening, and using Eq. (5)]. Note the sharply decreasing behavior of the transition rates calculated with analytical Dirac wave functions as Z approaches 137, and those calculated with DHF wave functions as Z approaches 170. (Mann reports that the K binding energy falls into the positron sea at $Z=172$.[15]) This behavior can be explained in the following way: As one approaches a stronger central field, the 1s wave function is pulled in closer and closer toward the nuclear center, while the L and M shell wave functions are not pulled in as fast. This means that the overlap between the K and outer-shell wave functions will begin to decrease, as will the integral over the overlap and spherical Bessel function, and hence the transition rate. [This was suggested to us by B. Müller, Universität Frankfurt/M (private communication).] Indeed, if one examines the integrals over the appropriate spherical Bessel functions in Eq. (5), it is evident that this is exactly what is happening.

Many other transition rates show this same maximal behavior. Table III gives a summary of our calculated radiative rates for filling vacancies in the K,L_1, L_2, and L_3 shells, and from this table, Figs. 2–7 were drawn to illustrate the predicted K x-ray spectra of these superheavy elements. The two lowest multipolarities are taken into account, for at high Z the electric dipole rates are no longer predominant over other multipoles. We have noted the occurrence of a maximum in the K-L_2 and K-L_3 rates, but other transition rates show an even more surprising behavior. For instance, the M_2 to K transition reaches a maximum at 130, decreases by two orders of magnitude, then starts to rise again and keeps rising up to $Z=170$. The N_2 to K transition does the same, as do the M_3-L_1, N_3-L_1, M_1-L_2, N_1-L_2, and M_1-L_3 transitions.

IV. DISCUSSION

What is the explanation for this extreme variation of rates with Z? We can see that the rate minima never occur for transitions for which the major component of both the upper and lower state lacks a radial node. Let us examine the details of contributions to the M_2 to K transition. We have ascertained three particular aspects: (a) that the entire quantity inside the large square brackets in Eq. (5b) changes sign between $Z=130$ and $Z=150$; (b) that if one computes the moments of r, i.e. $\int G_K G_{K'} r\, dr$ and $\int F_{K'} F_K r\, dr$, these two also change signs between $Z=130$ and 150; finally, (c) all of the results the unaffected if one uses Eq. (6) instead of Eq. (5b). The difference in the calculated transition rates are only a few tenths of a percent at most, and reflects an instability in the numerical integration more than anything else.

The significance of (b) is that it is the integral $\int G_K G_{K'} r\, dr$ that must be calculated to determine

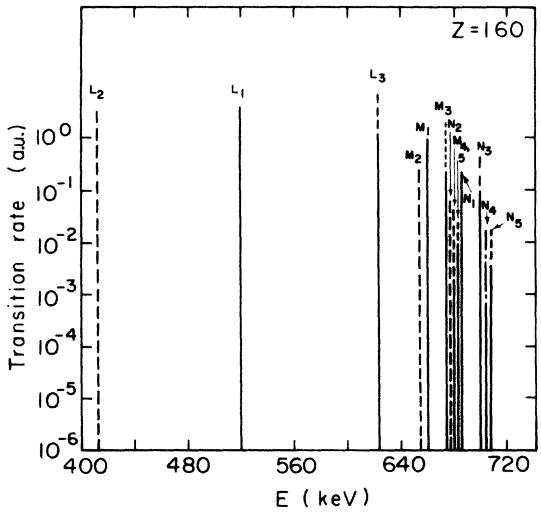

FIG. 6. Same as Fig. 2 for $Z=160$.

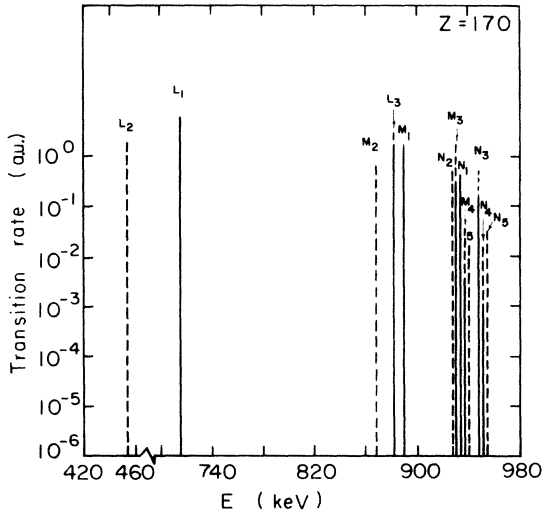

FIG. 7. Same as Fig. 2 for $Z=170$.

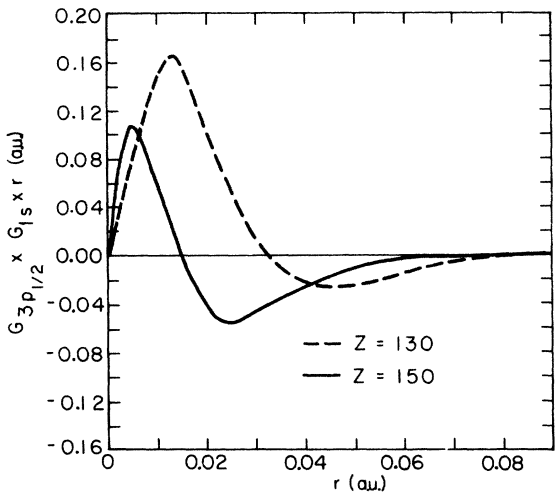

FIG. 8. Major component of the $3p_{1/2}$ (M_2) wave function multiplied by that for the $1s_{1/2}$ times r vs r for Z =130 and 150. Note the relative magnitude of the positive and negative lobes.

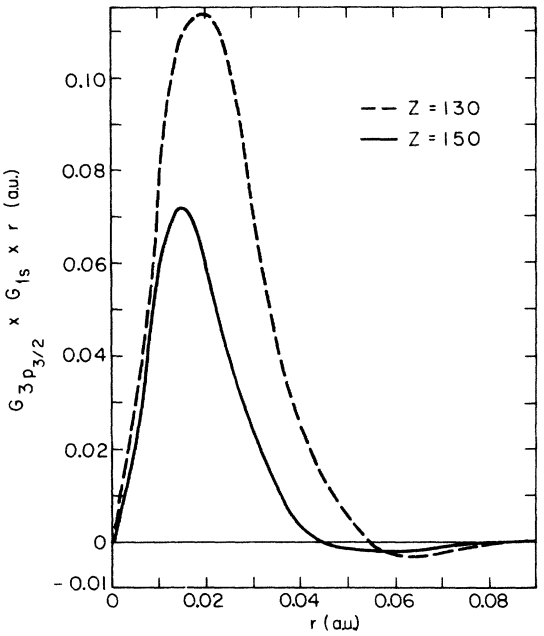

FIG. 9. Same as Fig. 8 for the $3p_{3/2}$ (M_3) wave function.

the dipole matrix element for the transition "nonrelativistically" i.e., by taking the nonrelativistic wave functions approximately as the major component G_κ. Figure 8 shows a plot of $G_{3p_{1/2}} G_{1s} r$ vs r and indicates why this change of sign occurs. The product has one node, and as the 1s wave function is pulled in closer and closer to the nucleus at higher Z, the area under the positive lobe decreases with respect to that under the negative lobe. The wave function $G_{3p_{3/2}}$ has a node as does the $3p_{1/2}$ wave function, so it is fair to ask why this same behavior does not occur there also. Figure 9 shows why. The node occurs at a larger value of r, where the G_{1s} wave function is much smaller; hence, the negative lobe of the product function is not as large as in the $3p_{1/2}$ case.

With these observations, it is not hard to see why the entire quantity inside the large square brackets in Eq. (5b) changes signs also, as one goes from Z = 130 to 150.

Lastly, it is interesting to speculate on the experimental observability of these transition rates at high Z. It is unfortunate that the kinds of united atom collisional radiation experiments that we mentioned earlier do not yield discrete peaks in x-ray spectra. Instead, one can only hope to observe a continuum extending from the x-ray peak of the heavier atom down to an end point which would correspond to the $K\beta_2'$ transition energy[21] of the united atom (UA). Previous experiments have not been able to unfold radiative lifetimes out of UA x-ray yields, due mostly to the complicated nature of the electron promotion processes going on inside their targets, and a myriad of other factors.

We would hope ultimately that the peaking in the total K transition rate might be reflected in the yield and spectral shape curves as united atom K x-ray studies are pushed from the present limit of Z_{UA} = 70 of Meyerhof *et al.*[21] on up to $Z_{UA} \geq 140$.

Of course much more research is needed on relativistic two-center molecular orbitals and other aspects of united atom x-ray production. It is hoped that this paper will stimulate these kinds of research.

ACKNOWLEDGMENTS

This work was supported by the AEC through the Yale Heavy Ion Accelerator Contract. The authors wish to thank Joe Mann at the Los Alamos Scientific Laboratory for sending us the wave functions used in this calculation and the Department of Computer Sciences at Yale University for the free use of their PDP-10 computer. In addition, one of us (R. A.) acknowledges fruitful discussions with Donald Beck in the Chemistry Department at Yale University; and appreciation for private communications from Berndt Müller at the Universität Frankfurt/M.

*Work performed under the auspices of the U. S. AEC.
†Present address: University of California, Lawrence Berkeley Laboratory, Berkeley, California 94720.
‡J. S. Guggenheim Fellow, 1973.

[1]B. Müller, J. Rafelski, and W. Greiner, Z. Phys. 257, 183 (1972).
[2]J. Rafelski, L. P. Fulcher, and W. Greiner, Phys. Rev. Lett. 27, 958 (1971).
[3]V. S. Popov, Sov. J. Nucl. Phys. 15, 595 (1972).
[4]P. H. Mokler, H. J. Stein, and P. Armbruster, Phys. Rev. Lett. 29, 827 (1972).
[5]H. E. Gove, F. C. Jundt, and H. Kubo, Bull. Am. Phys. Soc. 18, 559 (1973), and (private communication).
[6]W. B. Payne and J. S. Levinger, Phys. Rev. 101, 1020 (1956).
[7]G. R. Taylor and W. B. Payne, Phys. Rev. 118, 1549 (1960).
[8]F. A. Babuskin, Zh. Eksp. Teor. Fiz. 48, 561 (1965); [Sov. Phys.—JETP 21, 372 (1965)]; Acta Phys. Polon. 25, 749 (1964); Acta Phys. Polon. 31, 459 (1967).
[9]H. R. Rosner and C. P. Bhalla, Z. Phys. 231, 347 (1970).
[10]James Scofield, Phys. Rev. 179, 9 (1969).
[11]C. C. Lu, F. B. Malik, and T. A. Carlson, Nucl. Phys. A 175, 289 (1971).
[12]M. E. Rose, *Elementary Angular Momentum* (Wiley, New York, 1957).
[13]M. E. Rose, *Relativistic Electron Theory* (Wiley, New York, 1956).
[14]J. B. Mann and J. T. Waber, J. Chem. Phys. 53, 2397 (1970); At. Data 5, 201 (1973).
[15]J. B. Mann (private communication).
[16]T. A. Carlson, C. W. Nestor, F. B. Malik, and T. C. Tucker, Nucl. Phys. A 135, 57 (1969).
[17]R. L. Watson and J. O. Rasmussen, J. Chem. Phys. 47, 778 (1967).
[18]P. F. Dittner and C. E. Bemis, Jr., Phys. Rev. A 5, 481 (1972).
[19]S. I. Salem and C. W. Schultz, At. Data 3, 215 (1971).
[20]G. C. Nelson, B. G. Saunders, and S. I. Salem, At. Data 1, 377 (1970).
[21]W. E. Meyerhof, T. K. Saylor, S. M. Lazarus, W. A. Little, B. B. Triplett, and L. F. Chase, Jr., Phys. Rev. Lett. 26, 1279 (1973).